PAPER

NJC
www.rsc.org/njc

Zirconium organophosphonates as photoactive and hydrophobic host materials for sensitized luminescence of Eu(III), Tb(III), Sm(III) and Dy(III)†

Rita Ferreira,[ab] Preciosa Pires,[b] Baltazar de Castro,[a] Rute A. Sá Ferreira,[c] Luís D. Carlos[c] and Uwe Pischel*[a]

[a] *REQUIMTE, Departamento de Química, Faculdade de Ciências, Universidade do Porto, R. Campo Alegre, 4169-007 Porto, Portugal. E-mail: upischel@fc.up.pt; Fax: +35 1 22 608 2959; Tel: +35 1 22 608 2885*
[b] *ESTG, Instituto Politécnico de Viana do Castelo, Av. do Atlântico, 4900-348 Viana do Castelo, Portugal*
[c] *CICECO, Departamento de Física, Universidade de Aveiro, 3810-193 Aveiro, Portugal*

Received (in Montpellier, France) 5th July 2004, Accepted 8th September 2004
First published as an Advance Article on the web 15th November 2004

Novel luminescent materials based on lanthanides [Eu(III), Tb(III), Sm(III), and Dy(III)] and a mixed zirconium phenyl- and *m*-sulfophenyl phosphonate as the host matrix, have been prepared and photophysically characterized. Powder X-ray diffraction, ^{31}P-MAS-NMR spectroscopy, IR spectroscopy, and diffuse-reflectance UV spectroscopy revealed the specificity of these materials such as a layered structure, the presence of phenyl groups in the galleries, and the ability to absorb lanthanide ions introduced by simple ion exchange. Characteristic line-shaped long-lived luminescence [*ca.* 0.27 ms for Eu(III), 0.80 ms for Tb(III), and 0.05 ms for Sm(III)] was observed for different lanthanide ions, and was demonstrated to be generated by an antenna-induced energy transfer process to the metal. The overall luminescence quantum yield of europium- or terbium-loaded materials was measured to be *ca.* 0.3%. A detailed analysis of the Eu(III) luminescence spectrum and H_2O/D_2O exchange experiments indicated the presence of *ca.* 3 water molecules around each lanthanide. Based on the high maximum coordination numbers of lanthanides, up to 9 for free Eu(III) in aqueous solutions, and the presence of only monodentate sulfonate binding sites, more water could be expected. This observation is explained by the rather hydrophobic microenvironment in the interlamellar space of the materials, due to pendant organic moieties, that is, the phenyl groups.

Introduction

The luminescence of lanthanides (Ln) has been a focal point of photochemistry and its applications in recent years.[1–4] Because electronic transitions of lanthanides involve f orbitals, the absorption of light energy as well as its opposite pathway, the emission of photons, are parity-forbidden.[1] This causes very small molar extinction coefficients, generally lower than 1 M^{-1} cm^{-1}. On the other hand, due to the forbidden nature of the involved electronic transitions, excited state lifetimes are exceptionally long and generally in the hundreds of microseconds to several milliseconds range.[5] Emission spectra of lanthanides are line-shaped and cover a spectral range from the visible [Eu(III), Tb(III), Sm(III), Dy(III)] to the near-infrared region [Yb(III), Nd(III), Er(III)].[1] The almost unprecedented colour purity of light-emitting lanthanides, for example red for Eu(III) and green for Tb(III), finds its explanation in this special spectral feature.

The favourable luminescence properties of lanthanides have fostered their application in the development of chemosensors,[6–8] supramolecular devices such as logic gates,[9,10] bioassays (*e.g.*, for enzyme activity or DNA hybridization),[2] electroluminescent devices[4] or in optical telecommunication.[11] However, the application of lanthanide-based luminescence suffers from two serious drawbacks: (1) the aforehand-mentioned poor light absorption properties and (2) the efficient non-radiative deactivation of their excited states by OH oscillators such as water.[5] In order to avoid these obvious disadvantages for the application of lanthanides, a strategy has been developed that involves the so-called antenna effect (Scheme 1).[12] In this approach the lanthanide ion is linked *via* complexation with a ligand, which includes an organic chromophore capable of absorbing light energy with a higher efficiency than the metal itself. In a subsequent energy transfer process this chromophore acts as a sensitizer of the lanthanide excited state, which can subsequently deactivate through luminescence. Due to the large spectral gap between antenna excitation (often UV light) and emitted photons (visible to near IR), lanthanide-antenna conjugates have been often referred to as "molecular devices for wavelength conversion".[12] Furthermore, complexation with a ligand provides lanthanides with a certain degree of protection from surrounding water, hence increasing their luminescence quantum yields.

Numerous lanthanide-antenna conjugates operating *via* such an absorption–energy-transfer–emission sequence (A–EnT–E) have been generated, most of them in solution.[5,7–10,13,14] In order to allow technological processing of lanthanide-based luminescence, it is desirable to implement this sensitization

---

† Electronic supplementary information (ESI) available: experimental details for the synthesis of phenyl phosphonic and ***m***-sulfophenyl phosphonic acids; FTIR spectrum of ZrSPP; X-ray diffraction patterns of Na@ZrSPP and Ln@ZrSPP (Ln = Eu, Tb, Sm, Dy). See http://www.rsc.org/suppdata/nj/b4/b410222c/

DOI: 10.1039/b410222c

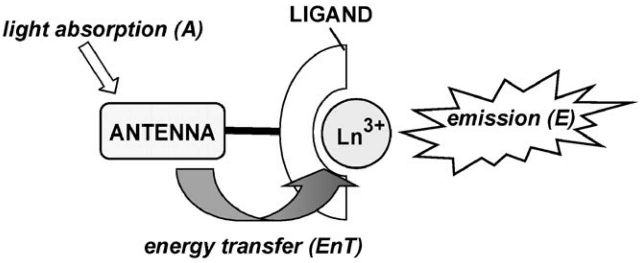

Scheme 1 Sensitization of lanthanide excited states by energy transfer from an antenna.

mechanism into solid state materials. Therefore, in recent years several efforts have been made to immobilize lanthanide-antenna systems in zeolites, sol-gel materials, and mesoporous MCM-41.[15–23] In the present contribution, we wish to report the synthesis of a layered material based on zirconium organophosphonates, capable of binding lanthanides and providing antenna functionality. Generally, zirconium phosphates and phosphonates form layered structures and by using conveniently modified organo-substituted phosph(on)ates as starting materials, it is possible to obtain inorganic-organic hybrid structures, which contain organic moieties in the galleries of the material.[24–27] The material's layer-to-layer distance depends on the size of the organic group, making it a key structural element.

The high versatility of this approach towards functionalized zirconium organophosph(on)ates has enabled the development of a variety of novel materials. In this context various photoactive components were integrated, such as for instance Os(II) and Ru(II) bipyridyl complexes,[28] fullerene or viologens as electron acceptors,[29,30] and aromatic chromophores (naphthalene, anthracene).[31] These materials and others, in which organic guests have been intercalated in zirconium phosphate phases,[32–35] have been proven to be useful to study electron transfer, energy transfer, and excimer formation in a solid host matrix.

The first studies using layered zirconium phosphates or phosphonates as host materials for lanthanides and their complexes were reported only recently. Lanthanide complexes were intercalated either in α-zirconium phosphate phases or in pillared γ-zirconium phosphates.[36,37] In the latter case polyethylenoxy chains served as pillars and were demonstrated to enhance the luminescence of europium and terbium *via* coordinative interactions.[37] In another report it was shown that uranyl ions served as sensitizers for europium luminescence, both being coordinated to carboxylate groups in the galleries of a zirconium carboxyethyl phosphonate.[38]

In this study we introduce a new luminescent zirconium phosphonate based on phenyl chromophores as antennae and several lanthanides [Eu(III), Tb(III), Sm(III), Dy(III)] as energy acceptors and luminescent entities. The emphasis of this contribution will lie on the exploration of the photophysical properties like luminescence lifetimes, quantum yields and influence factors like luminescence quenching by water. Several methods of structural characterization (PXRD, ^{31}P-MAS-NMR) and photophysical measurements (diffuse-reflectance UV spectroscopy, luminescence spectra, lifetimes, and luminescence quantum yields) allow us to present a comprehensive picture of lanthanide luminescence and its sensitization by an organic chromophore integrated into an inorganic architecture. Furthermore, our results point out the role of the hydrophobic effects exerted by organic residues in the galleries, which protect the lanthanides to a certain extent from water quenching.

Results and discussion

Preparation of a mixed zirconium *m*-sulfophenyl/phenyl phosphonate (ZrSPP)

A host material capable of sensitizing Ln luminescence *via* energy transfer should fulfil two conditions: (a) present an antenna chromophore and (b) present a lanthanide binding site, preferably in close proximity to the antenna. ZrSPP addresses both requirements by incorporating phenyl groups as antenna chromophores and sulfonic acid groups as potential ion exchange sites (Scheme 2).

To prepare a mixed zirconium *m*-sulfophenyl/phenyl phosphonate (ZrSPP), two phosphonate sources were synthesized: phenyl phosphonic acid and *m*-sulfophenyl phosphonic acid. Phenyl phosphonic acid was obtained from the oxidation of phenyl phosphinic acid by concentrated nitric acid. *m*-Sulfophenyl phosphonic acid was synthesized by reaction of phenyl phosphonic acid with chlorosulfonic acid. The preparation of ZrSPP was performed in aqueous solution by dissolving the corresponding phosphonic acid derivatives in water and adding dropwise a solution of zirconyl chloride. The material was formed immediately as a colourless precipitate. As mentioned beforehand, water is able to deactivate lanthanide luminescence through energy dissipation *via* OH vibrations. Therefore, we prepared a mixed *m*-sulfophenyl/phenyl phosphonate, to keep a moderate number of sulfonic acid groups and to provide a hydrophobic surrounding constituted by organic moieties, the phenyl groups, which should prevent the strong attraction of water into the galleries of the material (see below). This strategy has been successfully applied to synthesize hydrophobically shielded lanthanide complexes, where extensively phenyl-substituted imidodiphosphinates were used as ligands.[5] The resulting material, ZrSPP, was first ion-exchanged with sodium cations from a solution of NaOH + NaCl, and subsequently with the respective Ln ions from aqueous solutions of $LnCl_3$.

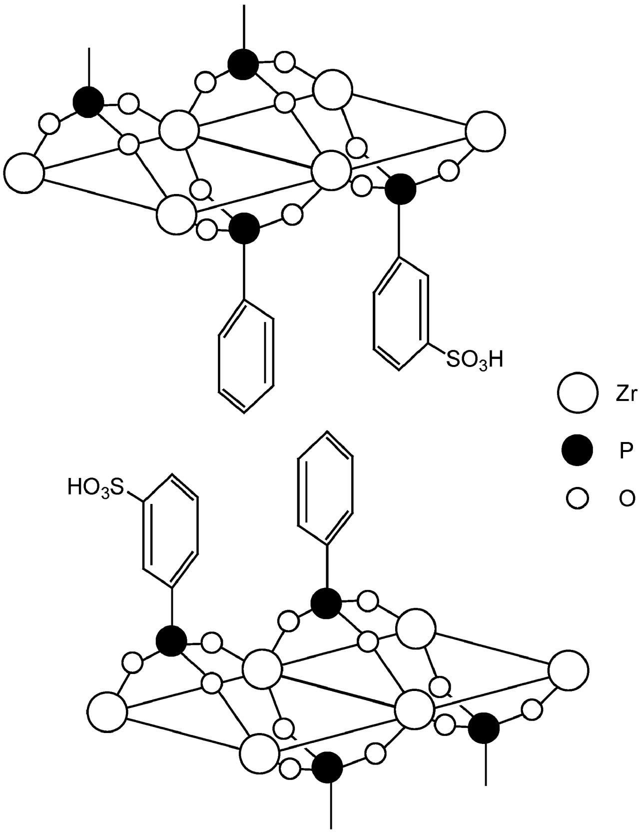

Scheme 2 Schematic representation of the layered structure of ZrSPP.

Materials characterization

Parent ZrSPP and the ion-exchanged materials Na@ZrSPP and Ln@ZrSPP (with Ln = Eu, Tb, Sm, Dy) were characterized by different techniques. Elemental analysis of the parent ZrSPP showed carbon and sulfur as indicators of the presence of the expected organic groups in the material. From the carbon-to-sulfur ratio it can be estimated that every fifth phenyl group carries one sulfonic acid function, leading to the general formula $Zr(O_3PC_6H_5)_{1.6}(O_3PC_6H_4SO_3H)_{0.4} \cdot nH_2O$. By thermogravimetric analysis, *ca.* 13 wt % water was determined from the weight loss up to 150 °C. This corresponds to n *ca.* 5.4. The thermal stability of the phenyl groups was investigated with the same technique, which indicated no appreciable decomposition of the organic content up to 450 °C. Only between 450 and 600 °C was notable weight loss observed due to degradation of the organic moieties.[39]

The lanthanide-ion-exchanged samples were analyzed by ICP-AAS or ICP-OES (which gave the same results within the error limits), to establish their Ln content. All materials were loaded to the maximum limit by using Ln salts in a large excess. Therefore, the final Ln content was practically the same for all materials (0.42 ± 0.02 mmol g^{-1} material). Only the Sm(III)-loaded sample had a slightly lower content with only 0.29 mmol Sm(III) g^{-1} material. All samples showed a residual content of unexchanged sodium (*cf.* Experimental). By comparing with the results obtained for sulfur by elemental analysis, that is, 0.53 mmol g^{-1} material, it can be estimated that every Ln ion corresponds to one sulfonate group. The other two positive charges of the trivalent Ln ions must be counterbalanced by other anions, most likely chlorides.

In order to further characterize the materials with regards to the presence of phenyl groups, the IR spectrum of ZrSPP was recorded (see Electronic supplementary information, ESI). Two regions were identified as belonging to the phosphonate PO_3 groups and to the phenyl rings. In the region between 900 and 1200 cm^{-1}, PO_3 stretching vibrations of the inorganic framework were detected. A strong band at 1149 cm^{-1} was ascribed to $P–C_6H_5$, based on the reported assignments for similar metal(IV) phosphonates.[40] Moreover, between 530 and 830 cm^{-1} the characteristic vibrations of phenyl rings could be observed and were assigned to mono-substituted (originating from phenyl phosphonate) and di-substituted (originating from *m*-sulfophenyl phosphonate) aromatic rings.

Three samples were investigated by ^{31}P-MAS-NMR spectroscopy as shown in Fig. 1. The most intense band of the sodium-loaded sample Na@ZrSPP was found at −4.9 ppm and corresponds to phosphonate groups bound to three Zr(IV) cations *via* non-protonated oxygen atoms.[39–41] The signal is well-shifted from that of free phenyl phosphonic acid, where the phosphorous resonance appears at +17.3 ppm; this situation is typically encountered in layered metal(IV) phosphonates.[41] Two smaller bands at 2.6 and 8.1 ppm were also detected and more likely originate from phosphorous only partly coordinated to Zr(IV) *via* some of the PO_3 oxygen atoms. Similar signals have been previously observed in the case of the related zirconium *p*-methylphenyl phosphonate.[42] In that case, cross-polarization experiments supported the assignment of these bands to phosphorous bound to free OH groups, which were not integrated into the zirconium phosphonate layers. By analogy, we suggest here the same assignment for the two minor signals observed. The Ln-exchanged samples Eu@ZrSPP and Tb@ZrSPP showed an equivalent signal at *ca.* −4.9 ppm with strong line broadening. At first glance, the absence of significant shifts of the signal is surprising, but it could be masked by the observed line broadening. When the fwhm of the signal was *ca.* 3 ppm in Na@ZrSPP, it was *ca.* 5 ppm in the Eu-loaded sample and even greater in the Tb-loaded ZrSPP with a fwhm at *ca.* 32 ppm. Furthermore, for the Ln-loaded materials, spinning side bands were more intense than in Na@ZrSPP. These effects are typical of paramagnetic lanthanides[1] and give firm evidence of their presence in the interlamellar space of the material.

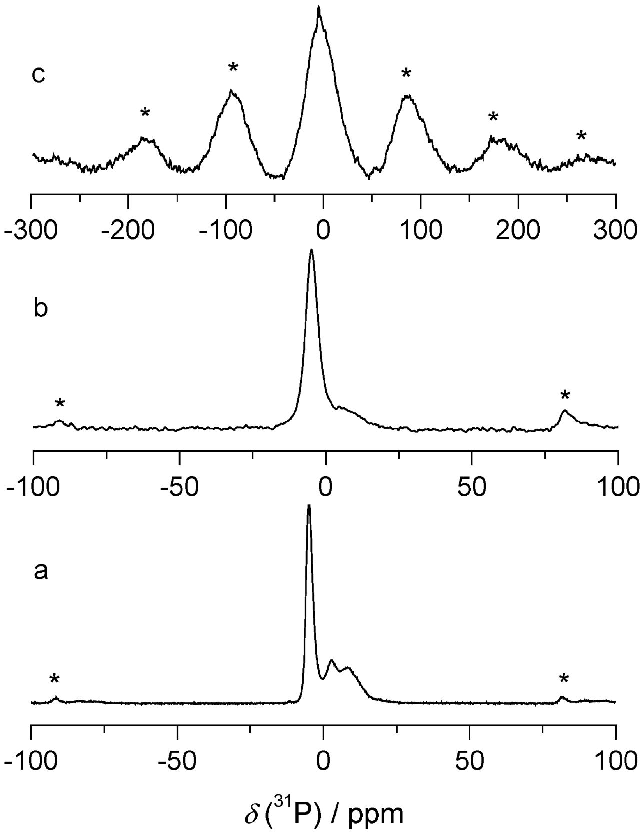

Fig. 1 ^{31}P MAS-NMR spectra of (a) Na@ZrSPP, (b) Eu@ZrSPP, and (c) Tb@ZrSPP. * marks spinning side bands.

The structures of Na@ZrSPP and the Ln-loaded ZrSPP were studied by powder X-ray diffraction (PXRD; see ESI) No sharp diffraction peaks were observed, which indicates the amorphous character of the zirconium organophosphonates. The layer-to-layer distances in the materials were estimated at 15–16 Å from the first reflection peaks. These estimated distances are in agreement with those measured in similar zirconium organophosphonates[43] and indicate the presence of space-filling phenyl groups in the galleries of the materials. For comparison, the layer-to-layer distance of zirconium phosphonate without organic groups is reported to be 5.6 Å, that is, lower than in the case of ZrSPP.[25] The layer-to-layer distance of Na@ZrSPP remains, in a first approximation, unchanged upon loading the material with different Ln ions.

The diffuse reflectance UV spectrum of ZrSPP (see Fig. 2, solid line) revealed two absorption bands at 221 and 265 nm, which can be assigned to π,π* transitions in the phenyl groups.[44] These absorption bands are absent in phenyl-free α-zirconium phosphate (α-ZrP) , which, instead, shows a much weaker band at 242 nm (see Fig. 2, dotted line). The latter is probably due to electronic defects in the structure as reported for phosphate glasses.[45]

Europium(III) and terbium(III) luminescence

Excitation of the phenyl groups at λ_{exc} = 275 nm gave rise to the typical luminescence spectra of lanthanides Eu(III) and Tb(III), Fig. 3. In the case of Eu@ZrSPP, bands at 594, 617 and 655 nm were observed in the emission spectrum. These bands have been previously assigned to $^5D_0 \rightarrow {}^7F_J$ transitions, with J = 1, 2 and 3, respectively (*cf.* Experimental).[1] The strong $^5D_0 \rightarrow {}^7F_2$ transition at 617 nm is responsible for the red colour of the luminescence. With Tb@ZrSPP, typical

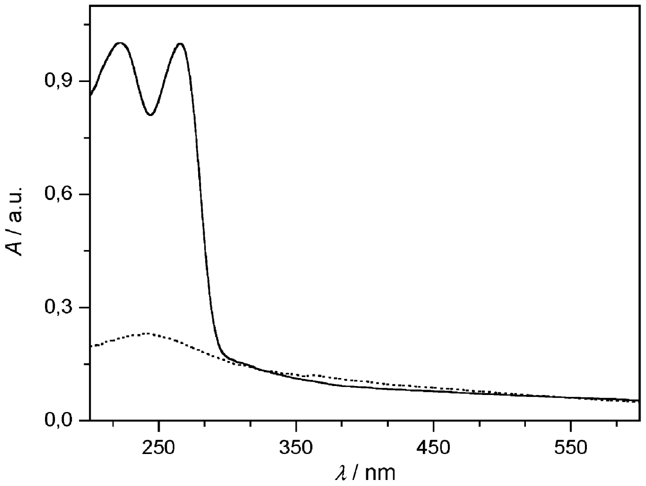

Fig. 2 Diffuse reflectance UV spectra of solid parent ZrSPP (solid line) and α-ZrP (dotted line).

emission lines at 490, 547, 590 and 624 nm were detected. These emission lines can be assigned to $^5D_4 \rightarrow {}^7F_J$ transitions, with J = 6, 5, 4 and 3, respectively. The strong band at 547 nm ($^5D_4 \rightarrow {}^7F_5$) is the origin of the green light emission.[1] All spectra are characterized by very narrow bands (fwhm *ca.* 10 nm), which are typical for lanthanide luminescence.

In order to prove that the detected luminescence is caused by energy transfer from excited phenyl antennae, excitation spectra were recorded (*cf.* inset Fig. 3), monitoring the emission wavelength at 617 nm for Eu(III) and 547 nm for Tb(III). The characteristic phenyl absorption band at *ca.* 265 nm was clearly identified. This demonstrates that the phenyl groups are able to act as antennae and constitutes an interesting example of energy transfer sensitization of Ln luminescence by an organic chromophore, which is an integral and structure-forming part of the inorganic-organic hybrid material. The excited triplet state of the antenna is generally the one involved in the energy transfer process.[46] The excitation energy of this state is not known for the phenyl groups in the material, but benzene is certainly a reliable model to use. The excited triplet state energy of benzene is 29500 cm^{-1},[44] well above the energy of the luminescent $^5D_0$ level of europium (17300 cm^{-1}) or the $^5D_4$ level of terbium (20500 cm^{-1}). In other words, antenna-to-lanthanide energy transfer is thermodynamically possible, as confirmed by our experimental observations. The emission characteristics of these samples were quantified and are compiled in Table 1. Both samples have practically the same overall luminescence quantum yield: $\Phi_{tot} \simeq 0.3\%$. This value seems to be quite low, but it must be kept in mind that the materials were prepared from aqueous solutions and therefore contain appreciable amounts of water, which can quench lanthanide luminescence Φ_{Ln} to a large extent.[1,5] However, other factors, also contributing to the overall luminescence quantum yield, are the efficiency of antenna intersystem crossing (η_{ISC}) and the efficiency of antenna-to-lanthanide energy transfer (η_{EnT}), which is distance dependent.[47,48] Eqn. (1) defines the overall luminescence quantum yield (Φ_{tot}) of the system as a function of these factors (with Φ_{abs} = quantum yield of light absorption):

$$\Phi_{tot} = \Phi_{abs} \times \eta_{ISC} \times \eta_{EnT} \times \Phi_{Ln}. \qquad (1)$$

Furthermore, the intrinsic lanthanide luminescence quantum yield Φ_{Ln} is defined in eqn. (2) by the competition between non-radiative processes (k_{nr}), that is, mainly water quenching, and radiative processes (k_r):

$$\Phi_{Ln} = \frac{k_r}{k_r + k_{nr}} \qquad (2)$$

In the case of europium luminescence the value of k_r can be estimated by spectral analysis with the help of eqn. (3):[18,49]

$$k_r = \frac{A_{0-1}\hbar\omega_{0-1}}{S_{0-1}} \sum_{J=0}^{4} \frac{S_{0-J}}{\hbar\omega_{0-J}} \qquad (3)$$

where J represents the final $^7F_{0-6}$ levels, S is the integrated intensity of the particular emission lines and ħω stands for the corresponding transition energies. A_{0-1} is the Einstein coefficient of spontaneous emission between the $^5D_0$ and the $^7F_1$ Stark levels. The branching ratios for the $^5D_0 \rightarrow {}^7F_{5,6}$ transitions must be neglected as they are too weak to be observed experimentally (*cf.* Experimental). Therefore, their influence can be ignored in the depopulation of the $^5D_0$ excited state. The $^5D_0 \rightarrow {}^7F_1$ transition does not depend on the local ligand field seen by Eu^{3+} ions and, thus, may be used as a reference for the whole spectrum, *in vacuo* A_{0-1} = 14.65 s^{-1}.[50] An average refractive index equal to 1.5 was considered, leading to $A_{0-1} \simeq 50$ s^{-1}.[51]

Appropriate analysis of the europium emission of Eu@ZrSPP according to eqn. (3) yielded a k_r value of 0.30 ms^{-1}. With the experimental lifetime of the $^5D_0$ state (τ_{exp} = 0.27 ms, *cf.* Table 1) the value of k_{nr} can be calculated ($1/\tau_{exp} = k_r + k_{nr}$) to be 3.40 ms^{-1}. Finally, with these rate constants, eqn. (2) gives an intrinsic europium luminescence quantum yield of $\Phi_{Ln} \simeq 8.1\%$. This value compares very well with those obtained for other europium-doped hybrid materials, for example, $\Phi_{Ln} \simeq 13\%$ for ureasil-europium nanocomposites or $\Phi_{Ln} \simeq 13.5\%$ for europium complexes of 3-hydroxypicolinic acid.[18,49] Instead of calculating k_r from the luminescence

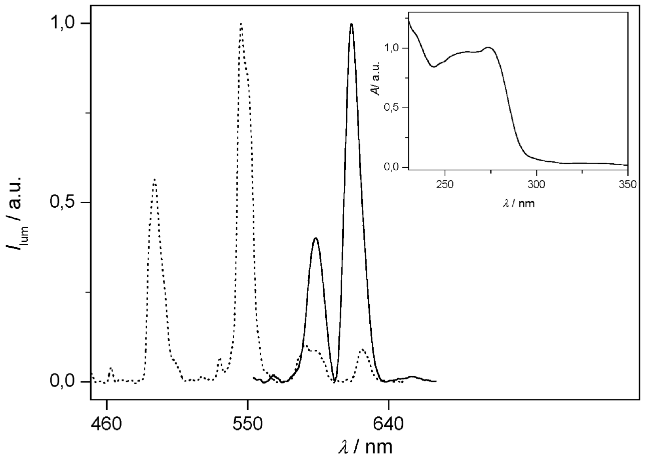

Fig. 3 Normalized emission spectra of solid Eu@ZrSPP (solid line) and Tb@ZrSPP (dotted line) at λ_{exc} = 275 nm. Inset: excitation spectrum of Tb@ZrSPP recorded at λ_{em} = 547 nm. The small peaks at 460 and 540 nm in the emission spectrum of Tb@ZrSPP are probably due to impurities.

Table 1 Photophysical parameters of Eu@ZrSPP and Tb@ZrSPP

	Eu@ZrSPP	Tb@ZrSPP
τ_{exp}/ms[a]	0.27	0.80
τ_{D_2O}/ms[b]	1.51	2.11
k_r/ms^{-1}	0.30[c]	0.47
k_{nr}/ms^{-1}	3.40	0.78
n_{H_2O}	3.9[d]	3.5[d]
Φ_{tot}	0.3	0.3
Φ_{Ln}[e]	0.081	0.376
η_{EnT}[e]	0.15	0.03

[a] Lifetime of the solid material [lifetime as an H_2O suspension: 0.23 ms for Eu(III) and 0.72 ms for Tb(III)]. [b] Measured as a suspension in D_2O. [c] Calculated with eqn. (3); value derived from the lifetime in D_2O: k_r = 0.66 ms^{-1}. [d] Calculated with eqn. (4) and parameters from ref. 55. See text for other values in the case of Eu(III). [e] See text.

spectra, the reciprocal lifetime of D_2O-exchanged samples can be used [k_r = 0.66 and 0.47 ms^{-1} for Eu(III) and Tb(III), respectively; see below]. According to these values and the reciprocal experimental lifetimes ($1/\tau_{exp}$), somewhat larger lanthanide luminescence quantum yields are estimated for both Eu@ZrSPP ($\Phi_{Ln} \simeq 17.8\%$), and Tb@ZrSPP ($\Phi_{Ln} \simeq 37.6\%$).

Now, eqn. (1) allows the calculation of the efficiency of antenna-to-lanthanide energy transfer processes in Eu@ZrSPP and Tb@ZrSPP. For this purpose the light absorption quantum yield (Φ_{abs}) is assumed to be unity and the intersystem crossing efficiency is taken from benzene as η_{ISC} = 25%.[52] Based on these assumptions, limiting values of $\eta_{EnT} \simeq 15\%$ for Eu(III) and 3% for Tb(III) for the energy transfer efficiency can be estimated. It has to be emphasized that lanthanides can exert a heavy atom effect, thereby increasing the intersystem crossing efficiency of the antenna in our materials, resulting in an even lower value for energy transfer efficiency. It is most likely that lanthanides are only close to the phenyl rings that present a binding sulfonate function (*ca.* 20% of all phenyl rings; see above), but in the majority, the antennae are much farther from the metals. This would naturally diminish the efficiency of energy transfer, as a function of the donor-acceptor distance,[48] accounting for the rather low values. The difference between Eu(III) and Tb(III) might be related to different spectral overlap, which is directly proportional to the energy transfer efficiency.[48]

From the above data (particularly the Φ_{Ln} and η_{EnT} values), it can be concluded that the presence of water in our materials contributes only to a certain extent to the diminution of the overall luminescence quantum yield (Φ_{tot}) and that an energy transfer of medium efficiency must be deemed responsible as well. However, although small in absolute value, the overall luminescence quantum yield of Eu@ZrSPP is comparable to other europium complexes with classical ligand systems, especially when ligand-to-metal charge transfer (LMCT) processes are possible.[5] For instance, in europium cryptate [Eu(III)$\subset$2.2.1], a total luminescence quantum yield comprised between 0.1 and 0.3% was measured.[53] In this context, it must be mentioned that terbium is not involved in LMCT, since its reduction potential does not favour charge transfer processes in general. In principal, low-lying LMCT states could also contribute to a diminution of the overall luminescence quantum yield of Eu@ZrSPP, thus explaining the comparably higher value of Φ_{Ln} in the case of Tb@ZrSPP (*cf.* Table 1).

Strikingly, the bare fact that luminescence is observed in our materials is remarkable, since their preparation has been done in aqueous solution and, furthermore, coordination of the lanthanide ions to sulfonate groups is not expected to offer sufficient protection from quenching by water molecules. Beside the estimation of the intrinsic luminescence quantum yield, excited state lifetime measurements can be used to obtain information on the presence of water in the coordination sphere of lanthanide ions. For both Eu@ZrSPP and Tb@ZrSPP materials, the decays, measured for the most intense luminescence band (*cf.* Fig. 4), could be fitted by mono-exponential functions. The lifetimes τ_{exp} were measured to be 0.27 ms for Eu@ZrSPP and 0.80 ms for Tb@ZrSPP. These values are similar to those reported for several lanthanide complexes immobilized in sol-gel materials, zeolites,[15,19] and lanthanide cryptates such as, for example, [Eu(III)$\subset$2.2.1], which has a lifetime of 0.31 ms in the solid state and 0.22 ms in water.[53] However, stronger protecting ligand systems lead to longer lifetimes, this accounting for the expected presence of coordinated water in our materials.[5] In order to estimate the number of water molecules coordinated to each lanthanide ion, we performed H_2O/D_2O exchange experiments. D_2O exchanges water and acts as a much weaker quencher, owing to the lower energy of the OD overtone vibrations compared to OH oscillators. As expected, lifetimes are much longer in D_2O suspensions, with values approaching up to 2.11 ms for Tb luminescence and 1.51 ms for Eu luminescence in Tb@ZrSPP and Eu@ZrSPP. For comparison, in [Eu(III)$\subset$2.2.1] a much shorter lifetime of 0.64 ms is obtained in D_2O,[53] pointing out the reasonable protection of lanthanides in our materials, albeit only a monodentate coordination with sulfonate groups is possible. The application of the corrected Horrocks equation,[54,55] eqn. (4):

$$n_{H_2O} = C \times (1/\tau_{exp} - k_r + \Delta k_{corr}). \qquad (4)$$

gives *n ca.* 3.5 ± 0.5 water molecules coordinated to each lanthanide ion in both materials. It is important to note that this number corresponds to an average of coordinated water molecules per lanthanide. It is expected that different lanthanide coordination modes may give rise to varying water access to the individual metal centres. In eqn. (4), *C* denotes an empirical constant [1.25 for Eu(III) and 4.90 for Tb(III)],[55] τ_{exp} is the experimental lifetime of Ln luminescence, Δk_{corr} is a correction term accounting for water quenching in the Ln second coordination sphere [−0.25 for Eu(III) and −0.06 for Tb(III)][55] and k_r is the radiative rate constant for the decay of the Ln excited state. k_r can be obtained by two ways: (a) from the analysis of the luminescence spectrum in the case of Eu@ZrSPP [*cf.* eqn. (3)] or (b) from a measurement of the lifetime in D_2O, according to the relation $k_r = 1/\tau_{D_2O}$. Method (b) has been often applied to lanthanide complexes in solution, but is very seldom used for solid state materials. The good agreement in the number of water molecules calculated by both methods for Eu@ZrSPP, that is, 3.9 ± 0.5 from the spectral analysis and 3.5 ± 0.5 from the H_2O/D_2O exchange, supports the applicability of the latter technique to solid state materials. Recently, Horrocks *et al.* reported another refined equation for the calculation of Eu-coordinated water [C = 1.11 and Δk_{corr} = −0.31 in eqn. (4)].[56] This equation was shown to yield results with smaller errors (±0.1 water molecules). Application of this relationship to Eu-loaded Eu@ZrSPP leads to 3.0 ± 0.1 and 3.4 ± 0.1 water molecules, with k_r obtained from D_2O exchange or spectral analysis, respectively. Based on the combined results we anticipate the number of water molecules for both Eu@ZrSPP and Tb@ZrSPP to be *ca.* 3.

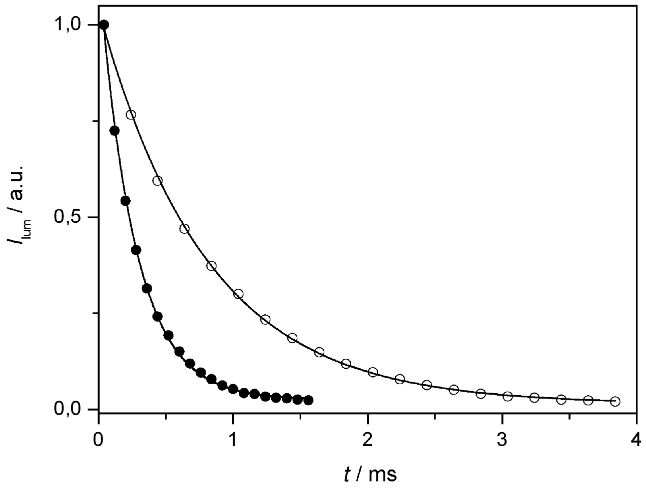

Fig. 4 Normalized luminescence decays of solid Eu@ZrSPP (full circles) and Tb@ZrSPP (open circles) and their respective mono-exponential fittings.

This number is noteworthy, since the coordination of Eu(III) and Tb(III) by a monodentate sulfonate and two other counterions, possibly chlorides, does not offer a high degree of protection. The values should be compared to the europium cryptate [Eu(III)$\subset$2.2.1], where 3.2 water molecules are coordinated (corrected to 3.1 using Horrocks' refined equation[56] and data from ref. 53), although the ligand offers seven donor binding sites.[53] Furthermore, it is well-known that free Ln ions in aqueous solutions can coordinate up to 9 water molecules, for example, 9.2 water molecules in Eu(III)$_{aq}$ in 0.5 M NaClO$_4$.[53] Therefore, this comparably low number of *ca.* 3 water molecules determined for our materials is quite surprising. A reasonable explanation is the limited water access in the galleries of the material due to the presence of hydrophobic phenyl rings. Even in a water suspension, the lifetimes are virtually the same (*ca.* 10% quenching) as in the solid state (*cf.* footnotes in Table 1). Hence, the lanthanide is protected by a rather hydrophobic microenvironment, similar to the reported cases of hydrophobic shielding by phenyl-substituted imidodiphosphinate ligands.[5] In this regard, studies of enzyme uptake by layered zirconium phenylphosphonate have provided ample evidence of the hydrophobic nature of the interlamellar space.[57] *Vice versa*, lanthanide luminescence can be also considered as a probe signal of the interlamellar space hydrophobicity.

Samarium(III) and dysprosium(III) luminescence

In order to demonstrate the capability of antenna-modified ZrSPP as sensitizers for lanthanides other than the commonly used europium and terbium, we extended our work to Sm(III) and Dy(III). Upon excitation at λ_{exc} = 275 nm, typical emission spectra were detected of D$_2$O suspensions of Sm@ZrSPP and Dy@ZrSPP (Fig. 5). In the case of Sm@ZrSPP, this corresponds to emission lines at 566, 602 and 647 nm, which are assigned to $^4G_{5/2} \rightarrow {}^6H_J$ transitions, with J = 5/2, 7/2 and 9/2 , respectively.[5] The strongest peak is the $^4G_{5/2} \rightarrow {}^6H_{7/2}$ transition at 602 nm. The emission spectrum of Dy@ZrSPP is composed of two intense lines at 484 and 577 nm, corresponding to $^4F_{9/2} \rightarrow {}^6H_J$ transitions with J = 15/2 and 13/2, respectively. The most intense emission line is at 484 nm.[5] Generally, the luminescence spectra of Sm(III)- and Dy(III)-loaded solids prepared from aqueous solutions were quite weak and were significantly enhanced by recording them as D$_2$O suspensions. Quantum yields are expected to be very small ($\ll$0.3% measured for europium- and terbium-loaded materials) and their measurements were therefore omitted. Occurrence of antenna-to-lanthanide energy transfer processes was supported by the match between excitation spectra and phenyl UV absorptions. As noted before for the energy transfer to Eu(III) and Tb(III), the excited state energy of the triplet antenna (29500 cm^{-1}) also lies well above the energy of the luminescent $^4G_{5/2}$ state of Sm(III) and the $^4F_{9/2}$ state of Dy(III), which are equal to 17900 and 21100 cm^{-1}, respectively.

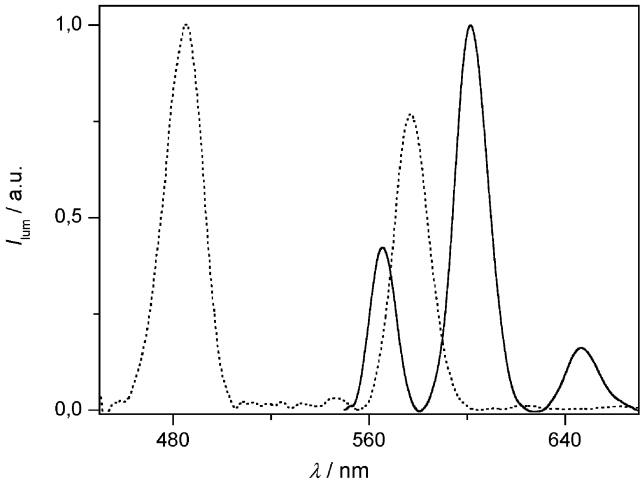

Fig. 5 Normalized emission spectra of Sm@ZrSPP (solid line) and Dy@ZrSPP (dotted line), recorded at λ_{exc} = 275 nm on D$_2$O suspensions.

The higher sensitivity of samarium- and dysprosium-derived luminescence towards water, in comparison to europium or terbium luminescence, can be explained by the energy gap between the excited luminescent states and the highest J levels of the ground states of these lanthanides. This energy gap is $\simeq$ 7500 cm^{-1} for Sm(III) and 7800 cm^{-1} for Dy(III), that is, considerably smaller than for Eu(III) and Tb(III) with values around 12300 cm^{-1} and 14800 cm^{-1}, respectively.[5] Since OH oscillators act independently (E_{vib} = 3657 cm^{-1}; symmetric OH stretching mode),[58] it can be estimated that, in the case of samarium and dysprosium, fewer water molecules are needed to bridge the gap than in the case of europium and terbium (*ca.* 2 *versus* 3–4). This higher water sensitivity explains why lifetimes of Dy(III) or Sm(III) luminescence are generally much shorter than those observed with Eu(III) or Tb(III), that is, tens of microseconds *versus* hundreds of microseconds to milliseconds. We tried to measure the lifetime of the Sm(III)-loaded ZrSPP with our setup, but it was apparently shorter than the pulse duration of the excitation source (<0.01 ms). In D$_2$O suspension, a longer lifetime of 0.052 ms was obtained, which is in the same range as for samarium complexes with imidodiphosphinate ligands in dry acetonitrile (0.15 ms)[5] or with a *m*-terphenyl derived tricarboxylate ligand measured in deuterated methanol (0.090 ms).[13]

Conclusions

A zirconium organophosphonate was used as host material for lanthanide absorption by simple ion exchange and allowed us to prepare novel luminescent solid state materials. The required antennae used to sensitize the long-lived Ln luminescent state are phenyl groups intimately implicated in the inorganic-organic hybrid architecture. It has been demonstrated that these aromatic rings are able to sensitize the excited luminescent states of a variety of lanthanide ions [Eu(III), Tb(III), Sm(III), and Dy(III)].

The Ln luminescence has been characterized by its overall quantum yield [Φ_{tot} *ca.* 0.3% for Eu(III) and Tb(III)] and lifetime [0.05 ms for Sm(III) suspended in D$_2$O, 0.27 and 0.80 ms for Eu(III) and Tb(III) in the solid state, respectively]. Since the materials were prepared from water solutions, the observation of long-lived lanthanide luminescence is striking. A detailed analysis of the intrinsic lanthanide luminescence quantum yield Φ_{Ln} (*ca.* 8–38%) and of the presence of coordinated water (*ca.* 3 water molecules per Ln) in the case of Eu@ZrSPP and Tb@ZrSPP points to a hydrophobic effect caused by the presence of organic groups in the galleries of the layered zirconium organophosphonate. Although the short lifetimes of Sm@ZrSPP and Dy@ZrSPPs luminescence did not allow us to measure them in the solid state, similar conclusions can be drawn based on analogy.

The photophysical data obtained for Eu(III) and Tb(III) in these materials compare very well with Ln ions complexed by cryptands, which are intrinsically expected to offer a higher protection of the Ln by providing more complexation sites.

Experimental

Chemicals

All chemicals used in the synthesis of the two organophosphonic acids and the preparation of the parent material (ZrSPP) were commercially available from Aldrich and Riedel de Haen, and were used as received without further purification. Lanthanide trichlorides in the hexahydrate form [Eu(III), Tb(III)] or as anhydrous salts [Dy(III), Sm(III)] were purchased from Aldrich (>99.9% purity). Sodium hydroxide and sodium chloride were purchased from Merck and used as received. Deuterium oxide (>99.5% D) was purchased from Aldrich. Phenyl phosphonic acid, commercially available from Aldrich, was synthesized in this work from phenyl phosphinic acid by oxidation with nitric acid (see ESI). *m*-Sulfophenyl phosphonic acid was prepared by sulfonation of phenyl phosphonic acid with chlorosulfonic acid in a standard procedure (see ESI). This compound has already been described in the literature.[59]

Material characterization

Elemental analysis of the precursors and Na@ZrSPP was performed by standard combustion techniques. Lanthanide and sodium contents of the materials were determined by induced coupled plasma–optical emission spectroscopy (ICP–OES, Kingston Analytical Services, UK), or atomic absorption spectroscopy (ICP–AAS, Laboratório Central de Análises, Universidade de Aveiro, Portugal). Two different methods were used to dissolve the samples leading, within error limits (10%), to the same results: (a) fusion with lithium metaborate followed by treatment with hydrofluoric acid and (b) digestion with H_2SO_4. Thermogravimetric measurements (TG) were performed in the temperature range of 25–650 °C (5 °C min^{-1}) with a thermoanalyzer Netzsch STA 409 EP. FTIR spectra were recorded on KBr pellets on a Jasco FTIR-460 spectrometer. Diffuse-reflectance UV/Vis (DR-UV/Vis) spectra were recorded on a Shimadzu UV/3101PC spectrophotometer with $BaSO_4$ reflecting standard. XRD measurements of the solid samples were performed on a Philips X'pert diffractometer, using CuKα radiation (λ = 1.540560 nm). ^{31}P magic-angle spinning (MAS) NMR spectra were recorded at 161.9 MHz, on an Avance 400 spectrometer, using 2 μs (45°) radio-frequency pulses, 60 s recycle delays and 14 kHz spinning rates. Chemical shifts are quoted in ppm and referred to 85% H_3PO_4.

Syntheses

Preparation of mixed zirconium *m*-sulfophenyl/phenyl phosphonate (ZrSPP). At room temperature, a solution of 9.03 g (27.5 mmol) of zirconyl chloride octahydrate in 60 ml of water was slowly added under stirring to a solution of 6.3 g (40.0 mmol) of phenyl phosphonic acid and 5.9 g (24.8 mmol) of *m*-sulfophenyl phosphonic acid in 60 ml of water. Immediately, a colourless precipitate was formed and, after centrifugation, the resulting gel was isolated and dried at 80 °C under vacuum for 72 h to yield 14.6 g of amorphous mixed zirconium *m*-sulfophenyl/phenyl phosphonate (ZrSPP). Elemental analysis: C 19.9%, S 1.7%. IR (KBr) in cm^{-1}: 1149 ($P–C_6H_5$), 1076 (PO_3), 1025 (PO_3), 804, 752, 728, 615, 560 (phenyl).

Sodium ion exchange (Na@ZrSPP). ZrSPP (3 g) was added to a solution of 60 mmol of sodium chloride and 21.6 mmol of sodium hydroxide in 80 ml of water. After stirring the mixture for 3 h, the solid was filtered off and washed with large volumes of water until the filtrate presented a neutral pH. The solid was finally dried at 80 °C.

Lanthanide ion exchange (Ln@ZrSPP). In a typical procedure, 0.7 mmol of lanthanide trichloride ($EuCl_3 \cdot 6H_2O$, $TbCl_3 \cdot 6H_2O$, $SmCl_3$ or $DyCl_3$) in 20 ml of water was added to 500 mg of Na@ZrSPP. The slurry was stirred overnight and thereafter the solid was filtered off, washed with large amounts of water and dried at 80 °C.

Lanthanide and sodium contents per gram of material (measurement technique in parenthesis): Eu@ZrSPP (ICP–OES): 0.43 mmol Eu, 0.14 mmol Na; Tb@ZrSPP (ICP–OES): 0.41 mmol Tb, 0.13 mmol Na; Tb@ZrSPP (ICP–AAS): 0.44 mmol Tb; Sm@ZrSPP (ICP–AAS): 0.29 mmol Sm; 0.01 mmol Na; Dy@ZrSPP (ICP–AAS): 0.41 mmol Dy, 0.04 mmol Na.

^{31}P MAS-NMR (85% H_3PO_4): δ for Na@ZrSPP: 8.1, 2.6, −4.9; Eu@ZrSPP: −4.9; Dy@ZrSPP: −4.8.

Photophysical measurements

Room temperature emission and excitation photoluminescence spectra and lifetime measurements were performed on Perkin Elmer spectrometers (LS50 or LS50B), equipped with a flashed xenon lamp (pulse width *ca.* 0.01 ms) and a 9781B model photomultiplier from Electron Tubes Ltd., UK, working in the range 165–680 nm. Therefore, the $^5D_0 \rightarrow {}^7F_4$ transition of europium at *ca.* 700 nm was not detected. For this reason, quantum yields and a highly resolved luminescence spectrum of europium were measured with a modular double grating excitation spectrofluorimeter with a TRIAX 320 emission monochromator (Fluorolog-3, Jobin Yvon-Spex) coupled to a R928 Hamamatsu photomultiplier. However, even with this fairly sensitive setup, the $^5D_0 \rightarrow {}^7F_{5,6}$ transitions were not detected. The spectra acquisition was done in front-face mode. Quantum yield measurements were performed according to the method by Wrighton *et al.*[60] using magnesium oxide as the reflecting standard. Spectral and lifetime measurements were performed with solid samples or in suspensions in D_2O or H_2O, as indicated in captions for figures and Table 1.

Acknowledgements

We thank Prof. J. Rocha (Universidade de Aveiro, Portugal) for recording the ^{31}P-MAS-NMR spectra and Dr A. Labrincha (Instituto Politécnico de Viana do Castelo, Portugal) for the thermogravimetric measurement.

References

1 J.-C. G. Bünzli and G. R. Choppin, *Lanthanide Probes in Life, Chemical and Earth Sciences – Theory and Practice*, Elsevier, Amsterdam, 1st edn., 1989.
2 H. Bazin, M. Préaudat, E. Trinquet and G. Mathis, *Spectrochim. Acta, Part A*, 2001, **57**, 2197–2211.
3 D. Parker, R. S. Dickins, H. Puschmann, C. Crossland and J. A. K. Howard, *Chem. Rev.*, 2002, **102**, 1977–2010.
4 J. Kido and Y. Okamoto, *Chem. Rev.*, 2002, **102**, 2357–2368.
5 S. W. Magennis, S. Parsons and Z. Pikramenou, *Chem.-Eur. J.*, 2002, **8**, 5761–5771.
6 A. P. de Silva, H. Q. Nimal Gunaratne, T. E. Rice and S. Stewart, *Chem. Commun.*, 1997, 1891–1892.
7 D. Parker, P. K. Senanayake and J. A. G. Williams, *J. Chem. Soc., Perkin Trans. 2*, 1998, 2129–2139.
8 L. J. Charbonnière, R. Ziessel, M. Montalti, L. Prodi, N. Zaccheroni, C. Boehme and G. Wipff, *J. Am. Chem. Soc.*, 2002, **124**, 7779–7788.
9 T. Gunnlaugsson, D. A. Mac Dónaill and D. Parker, *J. Am. Chem. Soc.*, 2001, **123**, 12 866–12 876.
10 M. de Sousa, M. Kluciar, S. Abad, M. A. Miranda, B. de Castro and U. Pischel, *Photochem. Photobiol. Sci.*, 2004, **3**, 639–642.
11 K. Kuriki, Y. Koike and Y. Okamoto, *Chem. Rev.*, 2002, **102**, 2347–2356.
12 J.-M. Lehn, *Supramolecular Chemistry – Concepts and Perspectives*, VCH, Weinheim, 1st edn., 1995.
13 M. P. O. Wolbers, F. C. J. M. van Veggel, B. H. M. Snellink-Ruel, J. W. Hofstraat, F. A. J. Geurts and D. N. Reinhoudt, *J. Chem. Soc., Perkin Trans. 2*, 1998, 2141–2150.
14 S. Petoud, S. M. Cohen, J.-C. G. Bünzli and K. N. Raymond, *J. Am. Chem. Soc.*, 2003, **125**, 13 324–13 325.
15 M. Álvaro, V. Fornés, S. García, H. García and J. C. Scaiano, *J. Phys. Chem. B*, 1998, **102**, 8744–8750.
16 V. Bekiari, G. Pistolis and P. Lianos, *Chem. Mater.*, 1999, **11**, 3189–3195.
17 Y. Wada, T. Okubo, M. Ryo, T. Nakazawa, Y. Hasegawa and S. Yanagida, *J. Am. Chem. Soc.*, 2000, **122**, 8583–8584.
18 R. A. Sá Ferreira, L. D. Carlos, R. R. Gonçalves, S. J. L. Ribeiro and V. de Zea Bermudez, *Chem. Mater.*, 2001, **13**, 2991–2998.
19 M. H. Bartl, B. J. Scott, H. C. Huang, G. Wirnsberger, A. Popitsch, B. F. Chmelka and G. D. Stucky, *Chem. Commun.*, 2002, 2474–2475.
20 R. J. P. Corriu, F. Embert, Y. Guari, C. Reyé and R. Guilard, *Chem.-Eur. J.*, 2002, **8**, 5732–5741.
21 H. R. Li, J. Lin, L. S. Fu, J. F. Guo, Q. G. Meng, F. Y. Liu and H. J. Zhang, *Microporous Mesoporous Mater.*, 2002, **55**, 103–107.

22 P. N. Minoofar, R. Hernandez, S. Chia, B. Dunn, J. I. Zink and A.-C. Franville, *J. Am. Chem. Soc.*, 2002, **124**, 14 388–14 396.
23 S. Hashimoto, S. Kirikae and S. Tobita, *Phys. Chem. Chem. Phys.*, 2002, **4**, 5856–5862.
24 G. Alberti, U. Costantino, S. Allulli and N. Tomassini, *J. Inorg. Nucl. Chem.*, 1978, **40**, 1113–1117.
25 M. B. Dines and P. M. DiGiacomo, *Inorg. Chem.*, 1981, **20**, 92–97.
26 A. Clearfield and Z. K. Wang, *J. Chem. Soc., Dalton Trans.*, 2002, 2937–2947.
27 E. Brunet, M. J. de la Mata, O. Juanes and J. C. Rodríguez-Ubis, *Angew. Chem., Int. Ed.*, 2004, **43**, 619–621.
28 F. Odobel, D. Massiot, B. S. Harrison and K. S. Schanze, *Langmuir*, 2003, **19**, 30–39.
29 E. Brunet, M. Alonso, M. J. de la Mata, S. Fernández, O. Juanes, O. Chavanes and J.-C. Rodríguez-Ubis, *Chem. Mater.*, 2003, **15**, 1232–1234.
30 L. A. Vermeulen, J. L. Snover, L. S. Sapochak and M. E. Thompson, *J. Am. Chem. Soc.*, 1993, **115**, 11 767–11 774.
31 J. C. Amicangelo and W. R. Leenstra, *J. Am. Chem. Soc.*, 2003, **125**, 14 698–14 699.
32 D. P. Vliers, R. A. Schoonheydt and F. C. de Schryver, *J. Chem. Soc., Faraday Trans. 1*, 1985, **81**, 2009–2019.
33 C. V. Kumar and A. Chaudhari, *J. Am. Chem. Soc.*, 1994, **116**, 403–404.
34 C. V. Kumar, Z. J. Williams and R. S. Turner, *J. Phys. Chem. A*, 1998, **102**, 5562–5568.
35 D. M. Kaschak, J. T. Lean, C. C. Waraksa, G. B. Saupe, H. Usami and T. E. Mallouk, *J. Am. Chem. Soc.*, 1999, **121**, 3435–3445.
36 Q. Xu, L. Fu, L. Li, H. Zhang and R. Xu, *J. Mater. Chem.*, 2000, **10**, 2532–2536.
37 E. Brunet, M. J. de la Mata, O. Juanes and J. C. Rodríguez-Ubis, *Chem. Mater.*, 2004, **16**, 1517–1522.
38 C. V. Kumar and A. Chaudhary, *Microporous Mesoporous Mater.*, 1999, **32**, 75–79.
39 G. Alberti, U. Costantino, M. Casciola, S. Ferroni, L. Massinelli and P. Staiti, *Solid State Ionics*, 2001, **145**, 249–255.
40 G. Guerrero, P. H. Mutin and A. Vioux, *Chem. Mater.*, 2001, **13**, 4367–4373.
41 A. Clearfield, D. M. Poojary, B. L. Zhang, B. Y. Zhao and A. Derecskei-Kovacs, *Chem. Mater.*, 2000, **12**, 2745–2752.
42 P. Pires, *Ph.D. Thesis*, University of Liverpool, Liverpool, UK, 1995.
43 J. L. Colon, C. Y. Yang, A. Clearfield and C. R. Martin, *J. Phys. Chem.*, 1990, **94**, 874–882.
44 H. G. O. Becker, *Einführung in die Photochemie*, Deutscher Verlag der Wissenschaften, Berlin, 3rd edn., 1991.
45 D. Ehrt, P. Ebeling and U. Natura, *J. Non-Cryst. Solids*, 2000 **263–264**, 240–250.
46 Recently, a rare example has been reported, where the excited singlet states of a dansyl chromophore and a lissamine dye chromophore have been proven to sensitize the excited state of neodymium(III). See: G.A. Hebbink, S. I. Klink, L. Grave, P. G. B. Oude Alink and F. C. J. M. van Veggel, *Chem. Phys. Chem.*, 2002, **3**, 1014–1018.
47 Energy transfer from the excited triplet antenna to the lanthanide is supposed to be proceeding *via* a Dexter mechanism, which shows an e^{-r} dependence on the distance r between energy donor and acceptor. Often, the involvement of Förster resonance energy transfer has been discussed, but it seems not very likely based on the small molar extinction coefficients of lanthanides and the resulting small spectral overlap integral of the Förster mechanism.
48 S. Speiser, *Chem. Rev.*, 1996, **96**, 1953–1976.
49 P. C. R. Soares-Santos, H. I. S. Nogueira, V. Félix, M. G. B. Drew, R. A. Sá Ferreira, L. D. Carlos and T. Trindade, *Chem. Mater.*, 2003, **15**, 100–108.
50 M. H. V. Werts, R. T. F. Jukes and J. W. Verhoeven, *Phys. Chem. Chem. Phys.*, 2002, **4**, 1542–1548.
51 M. F. Hazenkamp and G. Blasse, *Chem. Mater.*, 1990, **2**, 105–110.
52 S. L. Murov, I. Carmichael and G. L. Hug, *Handbook of Photochemistry*, Marcel Dekker, Inc., New York, 2nd edn., 1993.
53 N. Sabbatini, S. Dellonte, M. Ciano, A. Bonazzi and V. Balzani, *Chem. Phys. Lett.*, 1984, **107**, 212–216.
54 W. D. Horrocks and D. R. Sudnick, *Acc. Chem. Res.*, 1981, **14**, 384–392.
55 R. S. Dickins, T. Gunnlaugsson, D. Parker and R. D. Peacock, *Chem. Commun.*, 1998, 1643–1644.
56 R. M. Supkowski and W. D. Horrocks, *Inorg. Chim. Acta*, 2002, **340**, 44–48.
57 F. Bellezza, A. Cipiciani, U. Costantino and M. E. Negozio, *Langmuir*, 2002, **18**, 8737–8742.
58 *CRC Handbook of Chemistry and Physics*, ed. D. R. Lide, CRC Press, Boca Raton, FL, 80th edn., 1999.
59 G. Alberti, L. Boccali, M. Casciola, L. Massinelli and E. Montoneri, *Solid State Ionics*, 1996, **84**, 97–104.
60 M. S. Wrighton, D. S. Ginley and D. L. Morse, *J. Phys. Chem*, 1974, **78**, 2229–2233.